

Study and Modeling DNA-Preconcentration Microfluidic Device

*Viet-Bac Nguyen, Van-Sang Pham**

Hanoi University of Science and Technology - No. 1, Dai Co Viet, Hai Ba Trung, Hanoi, Vietnam

Received: May 05, 2020; Accepted: June 22, 2020

Abstract

In this study, to enhance diagnostic efficiency, we focus on the effect of ion concentration polarization (ICP), an electroosmotic (EO) flow, electrophoretic (EP) velocity, and the selective membrane length upon the DNA preconcentration. The study is conducted using the direct simulation of the ions and DNA transport in the electrokinetic system. The transport process is governed by the system of Poisson-Nernst-Planck-Navier-Stokes nonlinear equations. Obtained results show the preconcentrating DNA ability in microfluidic devices, simultaneously point out the impaction of the length of the microchannel and selective membranes on DNA plug position. Rely on these results, we proposed an experiment model to increase the efficiency of the DNA preconcentration.

Keywords: Poisson-Nernst-Planck-Navier-Stokes, electrokinetic, deoxyribonucleic acid preconcentration, ion concentration polarization, electroosmosis, electrophoresis.

1. Introduction

In recent years, there has been an increasing interest in on-chip biomolecule detection and analysis due to their salient advantages such as low sample volume, fast analysis time, automated processing, and high integrity. Many microfluidic devices based on the nonlinear electrokinetic phenomenon - ion concentration polarization (ICP) have been developed to preconcentrate biomolecular samples. Moreover, DNA preconcentration gets more and more attention due to the need for bio-applications in medicine development, cell analysis, and early cancer diagnosis, so on [1].

Recently, in our previous works, we proposed a new type of electrokinetic concentration device which has been developed in a microfluidic chip format [2]. This device allows efficient trapping and concentration of biomolecules by utilizing ICP inside multi-well structures. Additionally, our device helps to optimize the preconcentration performance and increase the reaction rate as well as the detection sensitivity of immunoassays. The formation of highly concentrated biomolecular plug results from the ion permselectivity of nanoporous membrane in combination with an electroosmotic flow that transports biomolecules from the anodic reservoir towards the ion depletion zone near the membrane, simultaneously, the DNA molecules move in the opposite direction due to the electrophoretic velocity [1]. The combination of these movements would keep DNA molecule in a stable position in the microchannel. Due to the low

sensitivity of existing microfluidic DNA electrophoretic separation, a number of preconcentration techniques have been developed to address this issue which includes bipolar electrode, ion-selective membrane [3-5]. We study an integrated system for charged membranes and microfluid channels to investigate the impaction of membranes on the preconcentration of DNA molecule, e.g., flat membranes. These architectures have drawn much attention not only due to the rich scientific content related to ICP phenomenon but also due to their potential applications in biomolecule sensing, e.g., enhance energy efficiency, shorten time-consuming for fabrication device sensor.

Dhopeswarkar and his co-workers used the EO flow to compute the convection term in Nernst-Planck equation by the Helmholtz-Smoluchowski equation [6]. This approach eliminates the Navier-Stokes equation from the mathematical description which questions the accuracy of simulation solver. In this study, we discretize the fully coupled set of Poisson-Nernst-Planck-Navier-Stokes (PNP-NS) equations using the finite volume method (FVM) to simulate electrokinetic transport in the microfluidic system illustrated in Fig.1 [7].

The present study demonstrates an electrokinetic concentration model that has ability to concentrate DNA in a microfluidic channel using flat selective membranes. We carried out a number of simulation cases with different external electric fields, different sizes of membranes, as well as testing the model in

*Corresponding author: Tel.: (+84) 966.633.683
Email: sang.phamvan@hust.edu.vn

different charged particles. The formation of ionic depletion zones at the membrane imposes exclusive forces on DNA molecules and influences on the effect of EO flow and EP velocity for the DNA preconcentration.

2. Microfluidic device and numerical model

2.1. Microfluidic device

In order to investigate the role of ICP in preconcentrating DNA, we consider a 2D model of perm-selective membranes integrated in a microchannel as depicted in Fig. 1. The membranes are located on sides wall of a channel, a voltage bias is remained between the channel ends, inlet and outlet, to drive charged species, ions and DNA molecules, through the channel.

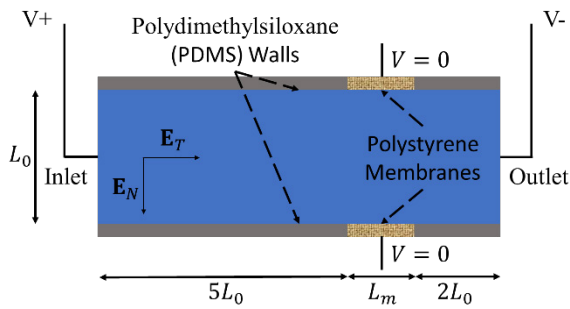


Fig. 1. The sketch of DNA preconcentration device.

The surface of permselective membranes have negative charge which allows positive ions (counterions) go through and repels the negative ions (co-ions) away from the membranes. This electrical interaction produces a phenomenon called ICP. Two main effects which represent for ICP are enrichment and depletion ion zone. The former is created at the anode side of permselective membrane, and the latter is formed at the other side. In this model, the depletion zone will be formed in the center of channel, between the two membranes.

The electrostatic interaction between the charged wall surface and the surrounding ions attracts the counter-ions and repels co-ions from the charged surface. As the result, a thin layer is formed with more counterions in the vicinity of the charged surface. This layer, called Electric Double Layer (EDL), is characteristic by Debye length λ_D (m)

$$\lambda_D = \sqrt{\frac{\epsilon_0 \epsilon_r k_B T}{e^2 N a C_0}} \quad (1)$$

where ϵ_0 is the permittivity of free space (C/Vm), ϵ_r is the relative permittivity of the material, k_B is the Boltzmann constant, T is the absolute temperature (K), e is the elementary charge (C), Na is Avogadro

number, Z is the magnitude of ion valence, and C_0 is bulk concentration (mol/m³) [1].

By applying a voltage difference ($V+$) at the inlet, a tangential electric field \mathbf{E}_T is generated along the microchannel (V/m). This electric field generates electric force which drives counterions in EDL along the field lines. The motion of fluid within the EDL pulls the bulk fluid along with it, produces an electroosmosis flow \mathbf{U}_{EO} (m/s)

$$\mathbf{U}_{EO} = -\frac{\epsilon_0 \epsilon_r \zeta_w}{\mu} \mathbf{E}_T \quad (2)$$

where $\zeta_w = \frac{\sigma_w \lambda_D}{\epsilon_0 \epsilon_r}$ is the zeta potential of a polydimethylsiloxane (PDMS) material (V), $\sigma_w = -0.0065$ is the charge density on the solid surface (C/m²), and μ is dynamic viscosity (Ns/m²) [8].

2.2. Transport of DNA in electrolyte solution

Diffusion of DNA is a kind of Brownian motion caused by thermal energy. As DNA molecules is relatively large compared with smaller molecules, there are several types of diffusion, including both translational diffusion and rotational diffusion. In this work, we focus on translational diffusion, i.e., diffusion of the center of mass of the DNA molecule. The translational diffusion is proportional to the thermal energy and thus proportional to $k_B T$.

Unlike hydrodynamic diffusion of DNA, Electrophoretic mobility of DNA, induced by Coulomb forces on the DNA charge, is reasonably well characterized by treating DNA as a free-draining polymer obeying Rouse dynamics under the assumption that the motion of water molecules in the region of the polymer is unaffected by the presence of the DNA molecule.

In the presence of electric fields, charged ions move in response to the Coulomb force – a process termed electrophoresis. The force exerted by an electric field makes the charged particles migrate along the field lines. The electromigratory velocity or EP velocity of particles caused by the electric field is written as

$$\mathbf{U}_{EP} = \mu_{EP} \mathbf{E}_T \quad (3)$$

where $\mu_{EP} = \frac{D_P Z_P}{\phi_0}$ is the electrophoretic mobility (m²/Vs), D_P is the diffusivity of a charged particle (m²/s), Z_P is particle valence [1].

The total velocity of particles is given by

$$\mathbf{U}_p = \mathbf{U} + \mathbf{U}_{EP} \quad (4)$$

where \mathbf{U} is the velocity of fluid (m/s).

We take into account the ICP, EO, EP phenomena in the mathematical model to investigate and design a microchannel that is able to concentrate the DNA molecules.

2.3. Mathematical model

In the system, ion transportation is governed by the Nernst-Planck Eqs.(5) and (6); the relationship between electric potential field and ion concentrations is demonstrated by Poisson Eqs.(7) and (8); and the fluid motion is described by the Navier-Stokes Eqs.(9) and (10). Dimensionless form of these equations is as follows:

$$\frac{1}{\tilde{\lambda}_D} \frac{\partial \tilde{C}_\pm}{\partial \tilde{t}} = -\tilde{\nabla} \cdot \tilde{\mathbf{J}}_\pm \quad (5)$$

$$\tilde{\mathbf{J}}_\pm = -\tilde{D}_\pm (\tilde{\nabla} \tilde{C}_\pm + Z_\pm \tilde{C}_\pm \tilde{\nabla} \tilde{\phi}) + Pe \tilde{\mathbf{U}} \tilde{C}_\pm \quad (6)$$

$$\tilde{\lambda}_D^2 \tilde{\nabla} \cdot (\tilde{\nabla} \tilde{\phi}) = -\tilde{\rho}_e \quad (7)$$

$$\tilde{\rho}_e = Z_+ \tilde{C}_+ + Z_- \tilde{C}_- \quad (8)$$

$$\frac{1}{Sc} \frac{1}{\tilde{\lambda}_D} \frac{\partial \tilde{\mathbf{U}}}{\partial \tilde{t}} = -\tilde{\nabla} \tilde{P} + \tilde{\nabla}^2 \tilde{\mathbf{U}} - Re (\tilde{\mathbf{U}} \cdot \tilde{\nabla}) \tilde{\mathbf{U}} - \frac{1}{\tilde{\lambda}_D^2} \tilde{\rho}_e \tilde{\nabla} \tilde{\phi} \quad (9)$$

$$\tilde{\nabla} \cdot \tilde{\mathbf{U}} = 0 \quad (10)$$

where \tilde{t} , \tilde{C}_\pm , $\tilde{\phi}$, $\tilde{\mathbf{U}}$ and \tilde{P} denote the dimensionless time, concentration of cations (+) and anions (-), electric potential, vector of fluid velocity, and pressure, respectively. These quantities are normalized by the corresponding reference values of time, ionic concentration, electric potential, velocity, and pressure, respectively as follow:

$$\tau_0 = \frac{L_0^2}{D_0}; C_0 = C_{bulk}; \Phi_0 = \frac{k_B T}{Ze} \quad (11)$$

$$U_0 = \frac{\varepsilon_0 \varepsilon_r \Phi_0}{\mu L_0}; P_0 = \frac{\mu U_0}{L_0}$$

where C_0 is the concentration scale (mol/m³), L_0 is the characteristic length scale (m), D_0 is the average diffusivity (m²/s), k_B is the Boltzmann constant, T is the absolute temperature (K), e is the elementary charge (C), and $Z = |Z_\pm|$ is ion valence. Parameters $\tilde{D}_\pm = D_\pm/D_0$, $\tilde{\lambda}_D = \lambda_D/L_0$, and $\tilde{\rho}_e = \rho_e/C_0$ are dimensionless diffusion coefficient, the Debye length, and the space charge, respectively. $Pe = U_0 L_0/D_0$, $Sc = \mu/\rho_m D_0$, and $Re = U_0 L_0 \rho_m/\mu$ are the Péclet number, the Schmidt number, and the Reynolds number, respectively [9].

To investigate DNA preconcentration process in microchannel devices under impaction of the electrical

force field and major ions in solution, we need to solve DNA transport equation:

$$\frac{1}{\tilde{\lambda}_D} \frac{\partial \tilde{C}_{DNA}}{\partial \tilde{t}} = -\tilde{\nabla} \cdot (-\tilde{D}_{DNA} (\tilde{\nabla} \tilde{C}_{DNA} + Z_{DNA} \tilde{C}_{DNA} \tilde{\nabla} \tilde{\phi})) + Pe \tilde{\mathbf{U}}_p \tilde{\nabla} \tilde{C}_{DNA} \quad (12)$$

where \tilde{C}_{DNA} , \tilde{D}_{DNA} , Z_{DNA} are concentration, diffusivity, and valence of DNA. To determine the diffusivity of DNA, we use empirical relations:

$$D_{DNA} \approx 3 \times 10^{-12} \times (l_c \times 10^6)^{-0.57} \quad (13)$$

where the contour length, l_c (m), is the arc length of the backbone contour and can be calculated approximately as

$$l_c \approx 0.34 \times 10^{-9} \times N_{bp} \quad (14)$$

with N_{bp} is the number of base pairs of DNA molecules [1]. The contour length l_c is the only molecular parameter that significantly affects DNA physical properties in aqueous solutions. As shown in Eq.(13), DNA's diffusivity is dependent on polymer length, i.e., the number of base pairs. Here, we simulated the preconcentration of DNA which has 25, 50, and 100 base pairs to find out the influence of electrophoresis on DNA transportation in the microchannel.

2.4. Boundary conditions

In order to close the Eqs.(5-10), the following boundary conditions were used:

At inlet and outlet boundaries, bulk ion concentration boundary $C_\pm = 10\text{mM}$; zero gradient boundary condition for DNA concentration; a voltage bias is remained between inlet and outlet to driven ion in the system.

At wall boundaries, Na^+ , Cl^- , DNA, and \mathbf{U} variables are enforced zero-value, while zero-gradient condition is applied for P and ϕ .

At membrane surface: the concentration of counterion, Na^+ , is fixed at the value of 15mM, the no-flux boundary condition is enforced for co-ion, Cl^- .

The concentration of ions and DNA was initially set at $C_\pm^{ion} = 10\text{mM}$, $C_{DNA} = 1\text{mM}$. Regarding the fluid flow, the no-slip boundary condition is enforced on the wall and membrane surface; the free-flow condition is assumed at inlet and outlet. The scales and dimensionless numbers, corresponding with above boundary conditions, are calculated below:

$$\tau_0 = 2.381e^{-1}(\text{s}); C_0 = 10(\text{mM}); L_0 = 20\mu\text{m}$$

$$\Phi_0 = 2.585e^{-2}(\text{V}); U_0 = 2.66e^{-5}(\text{m/s});$$

$$P_0 = 1.183e^{-3}(\text{N/m}^2); \lambda_D = 4.356e^{-9}(\text{m});$$

$$Pe = 0.317; Sc = 529.762; Re = 5.976e^{-4}$$

2.5. Numerical method

In this work, we employed the coupled method proposed by Pham to solve the sets of equations [9]. The finite volume method, a locally conservative method, is used for the discretization of the equations. The nonlinear discretized PNP equations are solved using the Newton-Raphson method [10]. To resolve the rapid variations of the ion concentrations and electric potential near charged surfaces, the mesh near the membrane is extremely refined toward the surfaces. To avoid solving the large system of linear equations and guarantee the strong coupling of the PNP equations, we make use of a coupled method for solving the sets of PNP and NS equations [9]. Starting with a velocity field from the previous iteration or initial condition, the potential and concentrations are simultaneously solved from the PNP equations. Then, electric body force is calculated and substituted into the NS equations. The velocity field obtained by solving the NS equations is substituted back into the PNP equations. The process is repeated until convergence is reached. The DNA equation is solved by coupling with the PNP-NS equations. We used GMSH to generate meshes [11]. Ratio between the largest and smallest cell is 1530.

We validated the accuracy of the numerical method by comparing the numerical solution to the analytical solution and solution published in the papers of electric potential on a solid surface interfacing with an electrolyte solution [12-13]. The potential can be calculated using the well-known Grahame equation,

$$\phi_{surface} = \frac{2k_B T}{e} \sinh^{-1} \left(\frac{\sigma_w}{(8\epsilon_0 \epsilon_r k_B T C_0 N a)^{1/2}} \right) \quad (15)$$

To examine the effect of mesh nonorthogonality on the simulation result, we consider two mesh types including an orthogonal mesh (consisting of rectangular control volume), a non-orthogonal mesh (consisting of triangular control volumes). Parameters used in the simulation include the bulk concentration with different values (0.1mM, 1 mM, 10mM), surface charge, temperature $T = 300\text{K}$, and the ion diffusivities.

The numerical and exact solutions for the surface potential at different bulk concentration are presented in Table 1. From the results, we can see a good agreement between the exact solution and the numerical solution for both orthogonal and non-orthogonal meshes. This agreement demonstrates the high accuracy of our numerical solution.

Table 1. The computed surface potential and ion concentration in comparison with published data.

C_{bulk} (mM)	$\phi_{computed}$ (mV)	$\phi_{computed}$ (mV)	$\phi_{computed}$ (mV)	ϕ (mV)	ϕ (mV)
		Orthogonal	Non-orthogonal	Mathur and Murthy [12]	Daiguji et al. [13]
0.1	-39.5	-39.52	-39.5	-39.58	-39.5
1	-13.5	-13.6	-13.62	-13.63	-13.7
10	-4.34	-4.35	-4.43	-4.42	-4.56

3. Results and discussion

In their experimental work, Kim and his co-workers used a microchannel with 1 cm in length at voltage 50V, this model generates the electric field of 5000 V/m [14]. In this study, we simulated a shorter microchannel with the smaller bias voltages to maintain the same electric field in the experiment. We simulated three cases with different lengths of membrane $L_m^1 = 1L_0, L_m^2 = 2L_0, L_m^3 = 5L_0$; the bias voltage ϕ applied at the inlet are $31\phi_0, 35\phi_0$, and $46\phi_0$, respectively (Fig.2). The dimensionless length of the microchannel is denoted as \tilde{L} . The number of cells in each case is 15504, 16864, and 19584, respectively. The red dashed lines present the selective membranes.

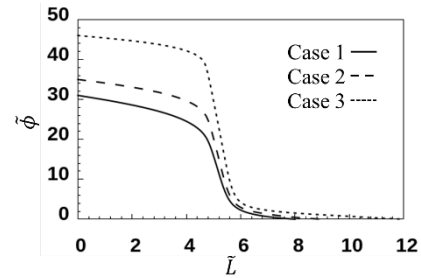


Fig. 2. The bias voltages along the microchannel.

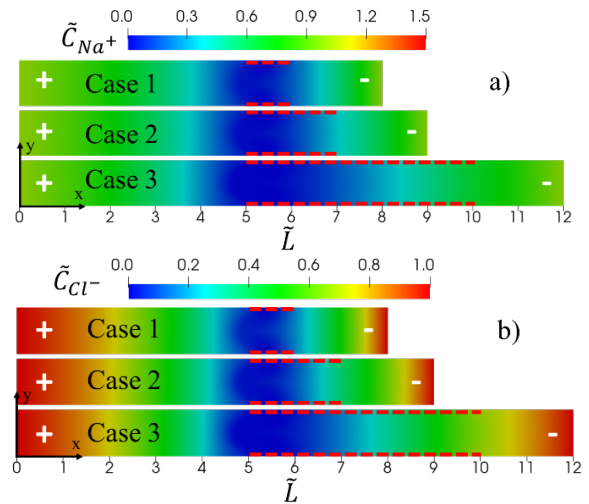


Fig. 3. The ICP at $\tilde{t} = 50T_0$ in microchannels.

3.1. Preconcentration phenomenon due to ion concentration polarization in microchannel

The tangential electric field along the anodic side of the microchannel generates EO flow, brings the target molecules into the region where they will be trapped by the ICP. Fig.3 shows the results of ICP inside a microchannel with an ion-selective membrane printed on the top and bottom of the channel. In Fig.2, the value of $\tilde{\phi}$ decreases rapidly due to the presence of charged membranes. The sharp decrease of voltage increases the value of the electric field \mathbf{E}_T along the channel. This electric field pulls the charged particles to the anode side of the channel. Therefore, the concentration of Na^+ (Fig.3a) and Cl^- (Fig.3b) decrease from the anode to the region where the selective membrane located and increase gradually to the value of bulk concentration (C_0) at the cathode. The depletion zone of ions forms between two sides of selective membranes and extends when increasing the voltage (Fig.4).

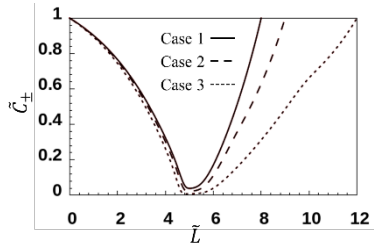


Fig. 4. The concentration of ions Na^+ and Cl^- along the microchannel.

3.2. Effect of membrane length on DNA preconcentration

As the selective membranes only allows cations to go through and repel the anions back to the solution, under the effect of electric field the space charge forms near the selective membranes as shown in Fig.5.

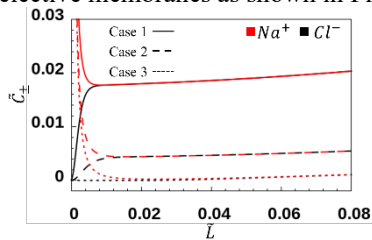


Fig. 5. The concentration of Na^+ and Cl^- near the selective membranes.

The bias voltage near the selective membrane increases rapidly (Fig.6) and generates the perpendicular electric field \mathbf{E}_N to the membrane which pushes the DNA out of this region. The higher voltage applied at the inlet results in a stronger \mathbf{E}_N .

The EO flow forms along the channel in all cases due to the zeta potential ζ_w and the tangential electric field \mathbf{E}_T (Eq.(2)). Because of the positive ions Na^+

move through the membrane, they push the fluid toward the impermeable membrane. As a result, a pair of vortex forms at the anode side of the membrane (Fig.7).

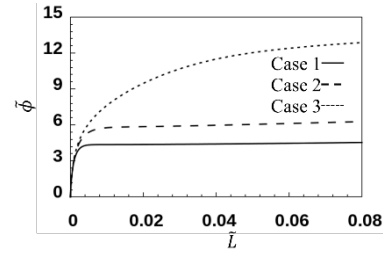


Fig. 6. The bias voltage near the selective membrane.

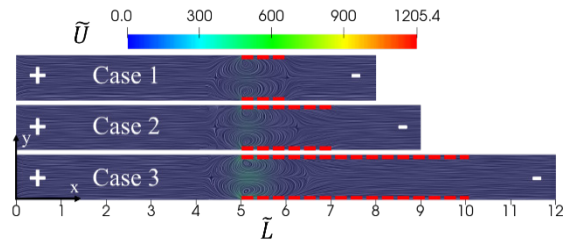


Fig. 7. The streamline of velocity at $\tilde{t} = 50T_0$.

In Fig.8, the EP velocity drags the preconcentration plug toward the anode side as the result of the negatively charge DNA. By increasing the length of the membrane, the position of DNA plug in case 3 is closer to the depletion zone than one in case 1.

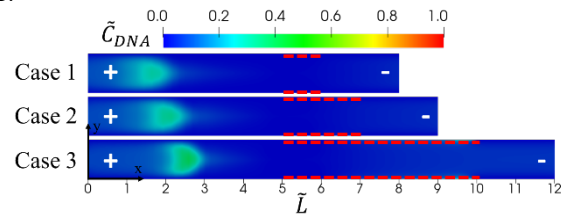


Fig. 8. The plug of DNA form in the microchannel at $\tilde{t} = 50T_0$.

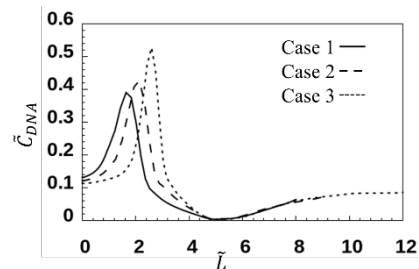


Fig. 9. The DNA concentration along the microchannel.

As can be seen from Fig.9, after $50T_0$ (s), the concentration of DNA increased ~ 5 fold corresponding to the bias voltage $\phi_{inlet} = 46\phi_0$. This result shows that with the same value of \mathbf{E}_T , the higher value of applying voltage and length of selective membrane, the higher value of DNA plug formed. In case 3, the DNA plug moves slowly to the anode side

of the selective membrane and decreases its value gradually (Fig.10).

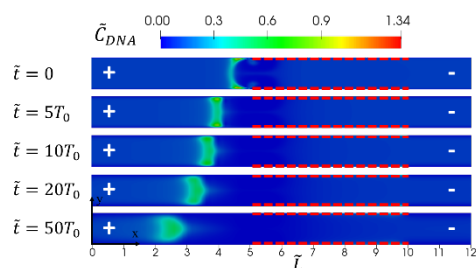


Fig. 10. The motion of DNA plug in case 3 over time.

3.3. Role of DNA charge on preconcentration

Due to the EP velocity influences directly on the charged particles in the electrolyte and electrophoretic velocity depends on the valence of a molecule so that we simulated three cases with different values of DNA valence, $Z_{DNA} = 50$, $Z_{DNA} = 100$, and $Z_{DNA} = 200$, respectively. The results show that the DNA molecules which have a higher value of valence will move faster and closer to the anode than one has a lower charge (Fig.11).

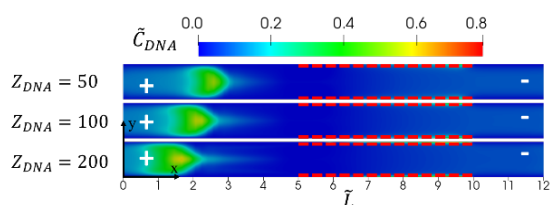


Fig. 11. The preconcentration of different DNA in the same microchannel.

4. Conclusion

In this study, by solving nonlinear PNPNS and DNA transport equations, we have analyzed transient electrokinetic of charged molecules in microchannels filled by the electrolyte solution. The important role of an electric field generates ICP phenomenon, EO flow, and EP velocity which preconcentrate DNA with ~ 5 fold of concentration inside the microchannel. We can control the position and value of the DNA plug by changing the length of the selective membranes and the channel. Moreover, with the different valence of DNA, the current models generate separate plugs of DNA. These peculiar results allow one to enrich and separate target analytes inside the microchannel. The above results are useful for optimizing designs of DNA preconcentration devices.

Acknowledgments

This research is funded by Vietnam National Foundation for Science and Technology Development (NAFOSTED) under grant number 107.03-2016.11

References

- [1] B. J. Kirby, *Micro- and Nanoscale Fluid Mechanics: Transport in Microfluidic Devices*, 536, Cambridge University Press, United States of America, first edition 2010.
- [2] X. Wei, V. Q. Do, S. V. Pham, D. Martins, and Y. A. Song, A Multiwell-Based Detection Platform with Integrated PDMS Concentrators for Rapid Multiplexed Enzymatic Assays, *Sci. Rep.* 8 1 (2018) 10772.
- [3] H. Song, Y. Wang, C. Garson, and Kapil Pant, Concurrent DNA preconcentration and separation in bipolar electrode-based microfluidic device, *Anal. Methods* 7 4 (2015) 1273–1279.
- [4] F. Mavre, R. K. Anand, D. R. Laws, K.-F. Chow, B.-Y. Chang, J. A. Crooks, and R. M. Crooks, Bipolar Electrodes: A Useful Tool for Concentration, Separation, and Detection of Analytes in Microelectrochemical Systems, *Anal. Chem.* 82 21 (2010) 8766–8774.
- [5] M. Jia and T. Kim, Multiphysics simulation of ion concentration polarization induced by a surface-patterned nanoporous membrane in single channel devices, *Anal. Chem.* 86 20 (2014) 10365–10372.
- [6] R. Dhopeswarkar, R. M. Crooks, D. Hlushkou, and U. Tallarek, Transient effects on microchannel electrokinetic filtering with an ion-permeable membrane, *Anal. Chem.* 80 4 (2008) 1039–1048.
- [7] F. Moukalled, L. Mangani, and M. Darwish, *The Finite Volume Method in Computational Fluid Dynamics - An Advanced Introduction with OpenFOAM and Matlab*, 817, Springer International Publishing Switzerland 113 2016.
- [8] R. J. Hunter, *Zeta potential in colloid science*, 391, Academic Press Inc., San Diego, third printing 1988.
- [9] V.-S. Pham, Z. Li, K. M. Lim, J. K. White, and J. Han, Direct numerical simulation of electroconvective instability and hysteretic current-voltage response of a permselective membrane, *Phys. Rev. E, Stat. Phys. Plasmas Fluids Relat. Interdiscip. Top.* 86 4 (2012) 046310.
- [10] J. E. Dennis and R. B. Schnabel, *Numerical Methods for Unconstrained Optimization and Nonlinear Equations*, 395, Prentice-Hall Inc., Englewood Cliffs, United States of America 1983.
- [11] C. Geuzaine and J.-F. Remacle, Gmsh: A three-dimensional finite element mesh generator with built-in pre- and post-processing facilities, *International Journal for Numerical Methods in Engineering* 79 11 (2009) 1309–1331.
- [12] S. R. Mathur and J. Y. Murthy, A multigrid method for the Poisson – Nernst – Planck equations, *Int. J. Heat Mass Transf.* 52 17–18 (2009) 4031–4039.
- [13] H. Daiguji, P. Yang, and A. Majumdar, Ion Transport in Nanofluidic Channels, *Nano Letters* 4 1 (2004) 137–142.
- [14] J. Kim, S. Sahloul, A. Orozaliev, V. Q. Do, V. S. Pham, D. Martins, X. Wei, R. Levicky, and Y.-A. Song, Microfluidic Electrokinetic Preconcentration Chips: Enhancing the detection of nucleic acids and exosomes, *IEEE Nanotechnol. Mag.* 14 2 (2020) 18–34